

R. R. Sonolikar, M. P. Patil, R. B. Mankar, S. S. Tambe and B. D. Kulkarni\*

# Genetic Programming based Drag Model with Improved Prediction Accuracy for Fluidization Systems

DOI 10.1515/ijcre-2016-0210

**Abstract:** The drag coefficient plays a vital role in the modeling of gas-solid flows. Its knowledge is essential for understanding the momentum exchange between the gas and solid phases of a fluidization system, and correctly predicting the related hydrodynamics. There exists a number of models for predicting the magnitude of the drag coefficient. However, their major limitation is that they predict widely differing drag coefficient values over same parameter ranges. The parameter ranges over which models possess a good drag prediction accuracy are also not specified explicitly. Accordingly, the present investigation employs Geldart's group B particles fluidization data from various studies covering wide ranges of  $Re$  and  $\varepsilon_s$  to propose a new unified drag coefficient model. A novel artificial intelligence based formalism namely *genetic programming* (GP) has been used to obtain this model. It is developed using the pressure drop approach, and its performance has been assessed rigorously for predicting the bed height, pressure drop, and solid volume fraction at different magnitudes of Reynolds number, by simulating a 3D bubbling fluidized bed. The new drag model has been found to possess better prediction accuracy and applicability over a much wider range of  $Re$  and  $\varepsilon_s$  than a number of existing models. Owing to the superior performance of the new drag model, it has a potential to gainfully replace the existing drag models in predicting the hydrodynamic behavior of fluidized beds.

**Keywords:** Fluidization, drag force, modeling, genetic programming, computational fluid dynamics

## 1 Introduction

The fluidized beds are versatile contactors employed in a wide range of chemical industries producing, for example, petroleum, food, and pharmaceuticals products. They are preferred in processes such as catalytic cracking of petroleum, and combustion and gasification of coals and biomasses. The preference for fluidized beds (FB) stems from their excellent heat and mass transfer, and solids mixing characteristics. These features are in turn related to the existence of bubbles and their behavior in the bed. In a fluidized bed, bubbles are responsible for mixing between various phases, circulation of fluid, and stabilization of temperature. Hence, understanding their transient behavior, and characteristics becomes essential. Especially, the knowledge of time averages of gas and solids velocities, void fraction, pressure, reaction kinetics, and catalytic influence is crucial for the design, operation, and optimization of a fluidized bed reactor. For many decades, the design of FB reactors was primarily dependent on the data from laboratory, bench-scale, and pilot plant scale experiments. Since these experiments are time and cost intensive to perform, design and operation of an FB reactor is also conducted by developing mathematical models based on the fundamental laws of mass, momentum, energy, and reaction conversion kinetics. An exhaustive literature on the modeling of fluidized beds and related concepts such as minimum fluidization velocity, bubble diameter, bubble velocity, bubble coalescence, splitting and slugging in the bed, particle velocity, flow pattern, and pressure distribution in and around the bubbles, is available in various books (Davidson and Harrison 1963, 1971; Kunni and Levenspiel 1991; Gibilaro 2001; Jackson 2000).

The Navier-Stokes equations have been widely used in modeling and designing of fluidized beds. With an exponential increase in the processing speeds of computers in the last few decades, the computational fluid dynamics (CFD) approach has gained a widespread

---

\*Corresponding author: **B. D. Kulkarni**, Chemical Engineering and Process Development Division, CSIR-National Chemical Laboratory, Dr. Homi Bhabha Road, Pashan, Pune 411008, India, E-mail: bd.kulkarni@ncl.res.in

**R. R. Sonolikar, M. P. Patil**, Solid and Hazardous Waste Management Division, CSIR-National Environmental Engineering Research Institute, Nehru Marg, Nagpur 440020, India

**R. B. Mankar**, Chemical Engineering Department, Laxminarayan Institute of Technology, Amravati Road, Ram Nagar, Nagpur, Maharashtra 440033, India

**S. S. Tambe**, Chemical Engineering and Process Development Division, CSIR-National Chemical Laboratory, Dr. Homi Bhabha Road, Pashan, Pune 411008, India

acceptance for the solution of Navier-Stokes fluidization models. There are two approaches for developing a CFD-based mathematical model for describing the fluidization phenomenon. The first one is known as *Eulerian-Eulerian* (“two-fluid” model), which considers both gas and solid phases as a continuum and assumes interpenetration of the phases via interphase momentum exchange. The second approach is termed *Eulerian-Lagrangian* that solves each particle’s motion individually, and considers the gas phase as a continuum.

In the present work, two-fluid model has been used for modeling gas and solid phases. It has been also used in most studies on gas-solid suspensions (Anderson and Jackson 1967; Du et al. 2006; Wang 2008). Here, Navier-Stokes equation is used for both phases since it considers each phase as an interpenetrating continuum. Among various terms of Navier-Stokes equation, the most influential one that significantly affects the bubble behavior (size, shape, velocity, coalescence and breakup) is the *interphase momentum exchange* term, usually referred as *drag*. Several theoretical/empirical models have been proposed based on experiments (Ergun 1952; Gidaspow and Ettihadieh 1983; Syamlal and O’Brien 1987) or data from Lattice Boltzmann simulations (Beetstra 2006; Beetstra, van der Hoef, and Kuipers 2007; Benyahia, Syamlal, and O’Brien 2006; Hill, Koch, and Ladd 2001; Khandai, Derksen, and Van den Akker 2003; van der Hoef, van sint Annaland, and Kuipers 2005) for the determination of the stated drag. Individually, these models can make reasonably accurate predictions of the bed expansion, bubble shape, and other gas-solid hydrodynamics in some regions of the parameter space. However, outside these regions – which are not always defined explicitly – the drag predictions of the existing models can be quite inaccurate. The predictions of different models also differ widely over same parameter ranges. Thus, the search for an improved model with a wider application potential has become an ongoing activity. Accordingly, in this paper, a novel artificial intelligence (AI) based exclusively data-driven modeling formalism, namely “genetic programming (GP),” has been adopted to propose a new drag model for Geldart type B particles possessing significantly higher prediction accuracy than the existing ones.

## 1.1 Existing drag models

The existing drag models for fluidized beds can be categorized in the following three groups:

(I) *Pressure drop based*: These models employ pressure drop across the fluidized bed wherein the

corresponding experimental data are analyzed for viscous and inertial regimes.

(II) *Terminal velocity based*: In this approach, terminal velocity of a single particle is modeled through a force balance, and it is extended for a multiparticle system.

(III) *Lattice Boltzmann simulation*: This serves as an alternative to solving Navier-Stokes equations. It uses statistical fluid dynamics for describing the flow behavior.

Several studies exist wherein performance of a number of drag models has been compared. Mckeen and Pugsley (2003) in their study on fluid catalytic cracking involving bubbling fluidized bed considered four drag models proposed by Gibilaro (2001), Gidaspow and Ettihadieh (1983), and Syamlal and O’Brien (1988) and found that the model predictions vary from the experimental results. Lundberg and Halvorsen (2008) compared drag models by Gidaspow and Ettihadieh (1983), Hill, Koch, and Ladd (2001), Syamlal and O’Brien (1988), Du Plessis (1994), and Richardson and Zaki (1954) and observed that their predictions of the bubble frequency matched reasonably well with those observed experimentally. Behjat, Shahhosseini, and Hashemabadi (2008) demonstrated that the model by Syamlal and O’Brien (1988) performed better than the model by Gidaspow and Ettihadieh (1983) in predicting the bed expansion and gas-solid hydrodynamics in a fluidized bed, although both models performed similarly in predicting the bubble shape. Hosseini et al. (2009) observed significant errors between the magnitudes of the experimental bed expansion ratios and those predicted by various drag models. By applying a suitable factor in the Gibilaro’s model, they could improve the accuracy of predictions pertaining to the bed hydrodynamics. Using *Multiphase Flow with Interphase eXchanges* (MFIx) software, Zinani, Philippsen, and Indrusiak (2013) studied the flow hydrodynamic in a bubbling fluidized bed wherein they investigated three drag models by Gidaspow and Ettihadieh (1983), Hill, Koch, and Ladd (2001), and Syamlal and O’Brien (1988). Here, Zinani and co-authors found that (a) for the models of Gidaspow and Ettihadieh (1983), and Hill, Koch, and Ladd (2001), the mesh independency was hard to achieve, and (b) the model by Syamlal and O’Brien, (1988) predicted smaller sized bubbles compared to those observed in experiments. This study also found a similarity between the shape predictions made by the models of Gidaspow and Ettihadieh (1983) and Hill, Koch, and Ladd (2001). In their study, Zimmermann and Taghipour (2005) modified the drag model by

Syamlal and O'Brien (1988) to get close to the experimental results. According to Li et al. (2008) the modified method is applicable over a limited range. Benzarti, Mhiri, and Bournot (2012) compared the drag models by Gidaspow and Ettihadieh (1983), Syamlal and O'Brien (1988), and Benzarti, Mhiri, and Bournot (2012) wherein it was observed that the first two models overestimated the drag by over-predicting the bed expansion. Additionally, it was found that the model by Benzarti, Mhiri, and Bournot (2012) predicts the drag better for 75 micron FCC (fluid catalytic cracking) particles. Yang et al. (2003) analyzed eleven drag models proposed by namely, Gibilaro (2001), Gidaspow and Ettihadieh (1983), Hill, Koch, and Ladd (2001), Syamlal and O'Brien (1988), Du Plessis (1994), Richardson and Zaki (1954), Esmaili and Mahinpey (2011), Wen and Yu (1966), Arastoopour, Pakdel, and Adewumi (1990), and Zhang and Reese (2003). In this analysis, none of the available drag models in their original form could make accurate predictions of the drag. Hence, Yang et al. (2003) modified the original model by Syamlal and O'Brien (1988) using the experimental minimum fluidization velocity and void fraction data. They also indicated that their model is superior to the other drag models. An overview of the drag models applied to fluidization can be found in De Felice (1994). From the above discussion it can be seen that at times there exists a significant variation in the  $\beta$  predictions of existing models.

The remainder of the paper is organized as follows. Section 2 first provides an overview of the GP formalism along with a brief account of the existing drag models. This section also details the CFD model describing the continuity and momentum balance equations as also the closure relations appropriate to the experimental set-up used in this study. Development of the GP-based drag model is described in Section 2.1, and the CFD model equations and their simulation conditions are given in Sections 2.2 and 2.3, respectively. Section 3 gives details of the setup used in conducting the fluidization experiments. Section 4 titled "Results and Discussion" provides results of the following four studies: (i) a comparison of the experimental fluidization snapshots with the corresponding CFD-simulated contours using the GP-based new drag model, (ii) a comparison of the drag coefficient magnitudes predicted by the GP-based model for wide ranges of Reynolds number and solid volume fraction values with those predicted by other drag models, (iii) a comparison of the experimental bed expansion ratio values with those predicted by the GP-based and other drag models, and (iv) a comparison of the experimental measurements of the steady-state pressure drop inside the

fluidized bed – as a function of the gas velocity – with the corresponding predictions made by the GP-based and other drag models. Finally, Section 5 summarizes the principle findings of this study.

## 2 Methods

### 2.1 Genetic programming (GP)

Genetic programming (Koza (1990); Enwald, Peirano, and Almstedt (1996); Poli, Langdon, and Mcphee (2008)) is an artificial intelligence (AI) based exclusively data-driven modeling formalism with several attractive properties. Specifically, it is a stochastic, population-based, and evolutionary search and optimization algorithm that follows Darwinian principles of natural selection and reproduction. It shares a number of features with an AI-based nonlinear optimization method termed *genetic algorithms* (GA) Holland (1975). Given an objective function, GA efficiently searches and optimizes values of the decision variables that would maximize or minimize the function. On the other hand, GP was introduced as a method for automatically generating computer programs that perform pre-defined tasks Poli, Langdon, and Mcphee (2008). There exists another novel GP application known as *symbolic regression* (SR), which is of interest to this study.

Given a set of example input-output data, the GP-based SR secures a function (expression/model) whose output satisfies a desired condition/property. Specifically, it searches and optimizes both, the specific form (structure) and the associated parameters of an appropriate linear/nonlinear data-fitting function. It is noteworthy that unlike the two widely employed AI-based data-driven modeling formalisms, namely, *artificial neural networks* (ANNs) and *support vector regression* (SVR), GP does not make any assumptions regarding the structure and parameters of the data-fitting function. The GP technique has been successfully used in a variety of modeling applications in chemistry and chemical engineering, for example, in the k-value prediction of crude oil Patil-Shinde et al. (2014), treatment of oily wastewaters Yi and Wanli (2011), assessment of soil liquefaction Fattah (2012) and compressibility factor Yang and Soh (2002), soft-sensor development Wang et al. (2008), estimation of higher heating value of biomass fuels Sharma and Tambe (2014), and coal gasifier modeling Holland (1975). The unique benefits of GP-based symbolic regression include (a) a human insight into and interpretability of the obtained models, (b)

identification of the key variables and their combination in the data, and (c) generation of expressions with reduced complexity for easy deployment into computational models Ghugare et al. (2014). In the following, the basics of the GP-based symbolic regression are described.

Consider a multiple input – single output (MISO) example dataset,  $D = \{x_i, y_i\} (i=1, 2, \dots, N_p)$ , consisting of  $N_p$  input-output patterns. Each input pattern/vector ( $x$ ) houses  $N$  elements ( $x = (x_1, x_2, \dots, x_N)^T$ ) and the corresponding scalar output is referred to as,  $y$ . The task of GP-based SR is to fit a suitable linear/nonlinear function ( $f$ ), which best fits the dataset,  $D$ :

$$y = f(x_1, x_2, \dots, x_N; \alpha_1, \alpha_2, \dots, \alpha_M) \quad (1)$$

where,  $\alpha$  represents an  $M$ -dimensional vector of function parameters,  $\alpha = [\alpha_1, \alpha_2, \dots, \alpha_M]^T$ . Towards searching and optimizing the structure/form of  $f$ , as also the associated parameters  $\alpha$ , GP begins by randomly generating a population of candidate solutions to the given function fitting problem. Each candidate solution (expression/function/model) in the population is represented in the form of a tree structure. In Figure 1(a), a tree structure representing

the expression “ $(x_2 - 9x_1) (5/x_3)$ ”, is illustrated wherein two branches emanate from the *root* node. Each node in these branches is randomly chosen to be either a ‘function’ or a ‘terminal’ node. The function node (also called an “operator node”) defines a mathematical operator that belongs to a set comprising, for instance, *arithmetic, trigonometric, inverse-trigonometric, exponentiation, and logarithmic* operators. The terminal (also termed “operand”) node represents an input variable ( $x_n$ ) or a function parameter ( $\alpha_m$ ). Tree structures vary in their depths and they can be easily evaluated in a recursive manner. The said variation in tree depths allows construction of candidate solutions of varying lengths and complexity.

A typical implementation of a generic GP comprises following steps: *initialization, fitness evaluation, selection, crossover* and *mutation*. Among these, the last four steps are performed iteratively until a best data-fitting linear/nonlinear candidate solution (expression) is obtained. The said procedure is repeated by systematically varying GP algorithmic parameters to secure an overall best data-fitting model. The flowchart of a generic GP procedure is provided in Figure 2.

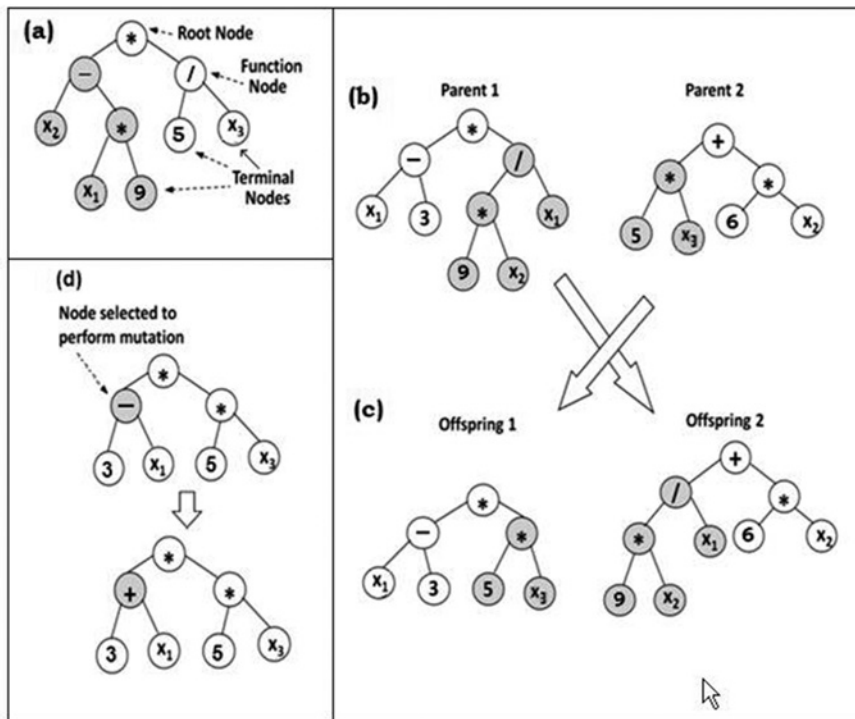


**Figure 1:** Schematic of a generic GP: (a) illustration of a tree structure representing “ $(x_2 - 9x_1) (5/x_3)$ ”, (b) random selection of branches for reproduction, (c) *crossover* operation, and (d) *mutation* operation. Symbols in the figure denote following operators (function nodes): (“+”) addition, (“-”) subtraction, (“\*”) multiplication, and (“/”) division; terminal (operand) nodes define inputs  $\{x_n\}$  and function parameters  $\{\alpha_m\}$ .

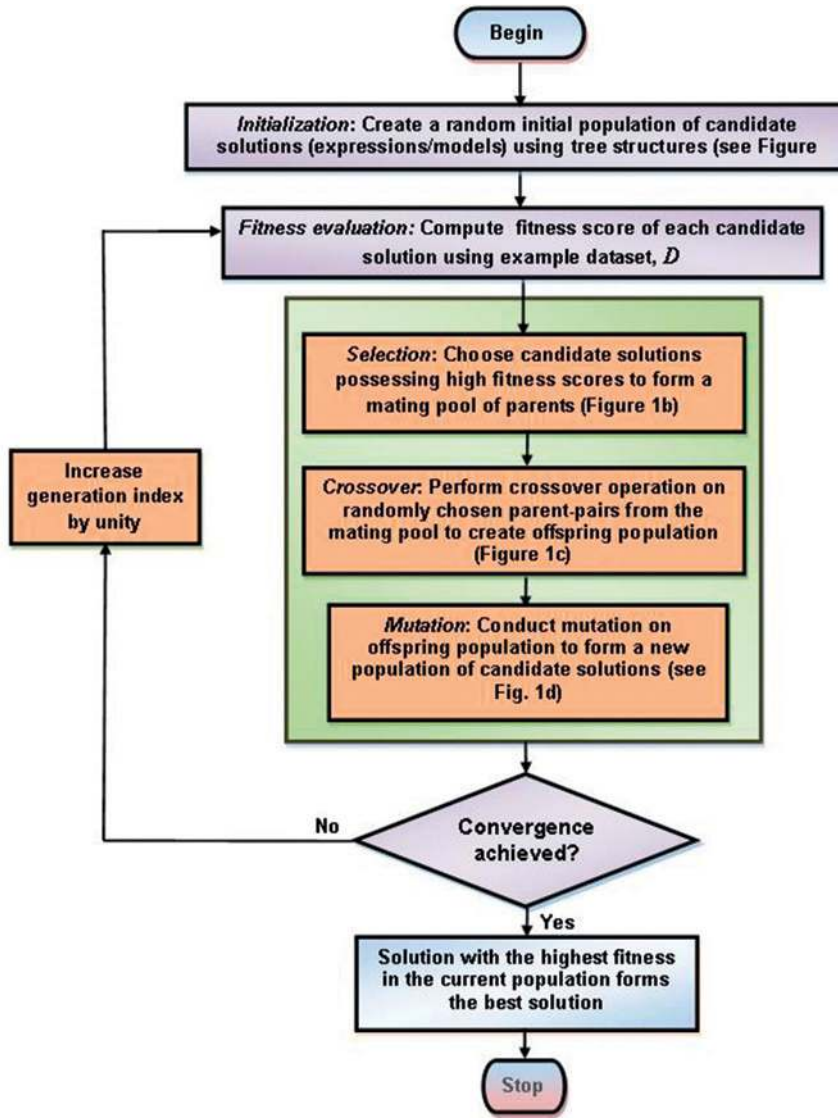


Figure 2: Flowchart of a generic GP-SR implementation.

Genetic programming implementation is a stochastic and not a deterministic procedure; hence, it is likely that repeated GP runs – for instance, using different random initializations – will lead to different converged solutions. Analysis of a set of several runs is therefore required to produce an acceptable model. An in-depth treatment of the GP procedure can be found, for example, in Enwald, Peirano, and Almstedt (1996), Kotanchek (2004), Wang et al. (2008), Sharma and Tambe (2014) and Shrinivas et al. (2016).

## 2.2 CFD model equations

The conservation equations of mass and momentum for gas phase (g) and solid phase (s) utilized in this study are given below.

Equations of Continuity

$$\frac{\partial(\varepsilon_g \rho_g)}{\partial t} + \nabla(\varepsilon_g \rho_g u_g) = 0 \text{ (Gas phase)} \quad (2)$$

$$\frac{\partial(\varepsilon_s \rho_s)}{\partial t} + \nabla(\varepsilon_s \rho_s u_s) = 0 \text{ (Solid phase)} \quad (3)$$

Momentum balance

$$\frac{\partial(\varepsilon_g \rho_g u_g)}{\partial t} + \nabla(\varepsilon_g \rho_g u_g u_g) = \nabla(\varepsilon_g \tau_g) - \varepsilon_g \nabla P + \varepsilon_g \rho_g g - \beta(u_g - u_s) \text{ (Gas phase)} \quad (4)$$

$$\frac{\partial(\varepsilon_s \rho_s u_s)}{\partial t} + \nabla(\varepsilon_s \rho_s u_s u_s) = \nabla(\varepsilon_s \tau_s) - \varepsilon_s \nabla P + \varepsilon_s \rho_s g + \beta(u_g - u_s) - \nabla p_s \text{ (Solid phase)} \quad (5)$$

Where  $\varepsilon_g$  and  $\varepsilon_s$  represent the volume fraction for gas and solid, respectively ( $\varepsilon_s + \varepsilon_g = 1$ ),  $P$  denotes pressure,  $p_s$  defines particle-particle interaction,  $\beta$  refers to the fluid-particle interaction coefficient (interphase momentum transfer coefficient), i. e. the drag coefficient,  $\rho$  is the density of particles, and  $\tau$  denotes the stress tensor.

### Closure modeling

Constitutive equations are required to close the governing equations of continuity and momentum. These are given in *Supplementary Material* as Table S.1. The various symbols appearing in the equations are defined in *Nomenclature*.

In this study, performance of the GP based drag model has been compared with a number of currently available drag models, which are tabulated in Table 1.

## 2.3 CFD simulation

In the present study, CFD simulations were performed for comparing the performance of the GP-based drag model with various other models available in the literature. The simulations carried out here involve systematic variations in two significant input parameters, namely, Reynolds number, and gas velocity, of the drag models, and studying their effects on the bubble behaviour and bed height. Here, three dimensional Cartesian coordinates were used; the walls were modeled as impermeable. To account for the particle wall interaction, specular coefficient magnitude of 0.1 was used Altantzis, Bates, and Ghoniem (2015). The gas distributor at the bottom of the bed was assumed to be a fluid phase influx wall. At the top of the bed a continuous outflow was assumed for the fluid and solid phases, respectively. Continuous outflow implies that

**Table 1:** Drag models used in the performance comparison of GP-based model.

No.	Drag model by	Drag Model
1	Gibilaro (2001)	$\beta = \left[ \frac{17.3}{Re} + 0.336 \right] \frac{\rho_g}{d_s}  \vec{u}_s - \vec{u}_g  \varepsilon_s \varepsilon_g^{-1.8}; Re = \frac{d_s  \vec{u}_s - \vec{u}_g  \rho_g \varepsilon_g}{\mu_g}$
2	Gidaspow and Ettihadieh (1983)	$\beta = \begin{cases} \frac{150 \varepsilon_s^2 \mu_g}{d_p^2} + \frac{1.75 \varepsilon_s \rho_g}{d_p}  u_g - u_s  \text{ if } \varepsilon_g < 0.8 \\ \frac{3}{4} \frac{\rho_g \varepsilon_s \varepsilon_g}{d_p} C_D  u_g - u_s  \varepsilon_g^{-2.65} \text{ if } \varepsilon_g \geq 0.8 \end{cases}$ Where $C_D$ is given as Rowe, McGillivray, and Cheesman (1979) $C_D = \begin{cases} \frac{24}{Re} (1 + 0.15 Re^{0.687}) \text{ if } Re < 1000 \\ 0.44 \text{ if } n Re \geq 1000 \end{cases}$ $Re = \frac{\varepsilon_g \rho_g d_p  u_g - u_s }{\mu_g}$
3	Syamlal and O'Brien (1988)	$\beta = \frac{3 \varepsilon_g \varepsilon_s \rho_g}{4 d_p v_r^2} C_d  u_g - u_s $ Where $C_d$ is given as Dallavalle (1948): $C_d = \left[ 0.63 + \frac{4.8}{\sqrt{\frac{Re}{v_r}}} \right]^2$ Where $v_r$ is given as Garside and Al-Dibouni (1977) $v_r = \frac{1}{2}  A - 0.06 Re  + \frac{1}{2} \left[ \sqrt{(0.06 Re)^2 + 0.12 Re (2B - A) + A^2} \right]$ $A = \varepsilon_g^{4.14}$ $B = \begin{cases} 0.8 \varepsilon_g^{1.28} \varepsilon_g \leq 0.85 \\ \varepsilon_g^{2.65} \varepsilon_g > 0.85 \end{cases}$
4	Du Plessis (1994)	$\beta = \frac{26.8 \varepsilon_g^3}{(1 - \varepsilon_g)^{\frac{3}{2}} [1 - (1 - \varepsilon_g)^{\frac{3}{2}}]^2} \frac{\varepsilon_s^2 \mu_g}{\varepsilon_g d_p^2} + \frac{\varepsilon_g^2}{[1 - (1 - \varepsilon_g)^{\frac{3}{2}}]^2} \frac{\varepsilon_s \rho_g}{d_p}  u_g - u_s $
5	Arastoopour et al. (1990)	$\beta = \left[ \frac{17.3}{Re} + 0.336 \right] \frac{\rho_g}{d_s}  \vec{u}_s - \vec{u}_g  \varepsilon_s \varepsilon_g^{-2.8}; Re = \frac{d_s  \vec{u}_s - \vec{u}_g  \rho_g}{\mu_g}$
6	De Felice (1994)	$\beta = \frac{3}{4} C_D \frac{\varepsilon_s \rho_g}{d_p}  u_g - u_s  f(\varepsilon_s) f(\varepsilon_s) = \varepsilon_g^{-x} X = 3.7 - 0.6 \exp \left( -\frac{1}{2} (1.5 - \log_{10} Re)^2 \right)$

the fluid leaves the bed at its own chosen rate with a minimal upstream flow disturbance. The initial bed height was identical to the experimentally determined bed height at the minimum fluidization condition. A freeboard area of 54% was provided for the bed expansion and the simulations did not assume symmetry of fluidized bed.

The governing eqs (2) to (5) were solved by using (Commercial software FLUENT 14.5) the finite volume method. The grid size of eight times the particle diameter was used in simulations Altantzis, Bates, and Ghoniem (2015), Gelderbloom, Gidaspow, and Lyczkowski (2003). The computational domain was discretized into 635,635 rectangular cells and a time step of 0.001 sec was used in the simulation. The relative error between the successive iterations was specified by using a convergence criterion for each stated residual component, such as pressure, and velocities of gas and solid. A scheme known as *Quadratic Upstream Interpolation for Convective Kinematics* (QUICK) (Iaccarino 2001; Loha, Chattopadhyay, and Chatterjee 2012) was utilized for the discretization of governing equations. Time discretization was done using a first order scheme. The *Semi-Implicit method for Pressure-Linked Equations* (SIMPLE) (Iaccarino 2001; Loha, Chattopadhyay, and Chatterjee 2012) was applied for the correction of pressure and velocity. The linearized equations were solved using a block algebraic multi-grid model method (Esmaili and Mahinpey 2011). Table 2 summarizes the model parameters/conditions used in the CFD simulation of the 3D fluidized bed.

### 3 Experimental Set-up

In this study, experiments were conducted to validate and compare the performance of the proposed GP-based drag coefficient model. Figure 3 shows a three-dimensional fluidized bed that was constructed to study the formation and travel of bubbles in a gas-solid fluidized bed. This bed has a cross-section of 15 cm, height of 100 cm, and depth equal to 1.3 times the width. A porous plate was used for the distribution of gas, which yielded a pressure drop of 15% in the fluidized bed. The plenum has dimensions of 20 cm (width) x 3 cm (depth) x 30 cm (height). It was packed up to the height of 15 cm for uniform distribution of the gas. The flow rate of the fluidizing media (air) was accurately measured through a set of four rotameters covering a range of 0–200 lit/min. Spherical glass beads with a size distribution of 250–300 microns and density of 2,500 kg/m<sup>3</sup> were fluidized using air as

**Table 2:** Magnitudes of model parameters used in CFD simulations of 3D fluidized bed.

Sr. No.	Parameters	Value
1.	Particle density	2,500 (kg/m <sup>3</sup> )
2.	Gas density	1.2 (kg/m <sup>3</sup> )
3.	Mean particle diameter	0.000275 (m)
4.	Initial solid packing	0.55
5.	Superficial gas velocity	0.35 ... (m/s)
6.	Bed dimension	0.15 × 1.0 × 0.013 (m)
7.	Static Bed height	0.4 (m)
8.	Inlet boundary condition type	Velocity-inlet
9.	Outlet boundary condition type	Pressure-outlet
<b>Time Stepping Parameters</b>		
10.	Time stepping type	Fixed
11.	Time step size	0.001 (s)
12.	Number of time steps	15,000
13.	Max number of iterations per time step	20
<b>Under-relaxation factors</b>		
14.	Pressure	0.5
15.	Density	1
16.	Momentum	0.2
17.	Volume fraction	0.4
18.	Granular temperature	0.2
19.	Specularity coefficient	0.1
<b>Mesh Parameters</b>		
19.	Mesh type	Equi-spaced quadrilateral
20.	$\Delta x$	0.002 (m)
21.	$\Delta y$	0.002 (m)
22.	$\Delta z$	0.002 (m)
23.	Total number of cells	635,635

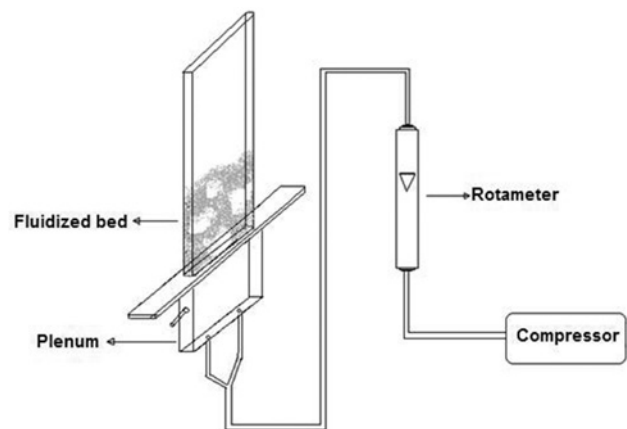


**Figure 3:** Schematic of the experimental fluidized bed.

the fluidizing medium. The static bed height of 0.4 m and solid volume fraction of 0.6 were used for obtaining the data for studying the bed height and bubble

behaviour. In the experiments, gas velocity was maintained at 0.21 m/s.

## 4 Results and discussion

### 4.1 Development of GP-based drag model

For developing the GP-based drag model predicting the magnitude of drag ( $\beta$ ) ( $\text{kg/m}^3\text{s}$ ), five fluidization related parameters, namely, *Reynolds number* ( $Re$ ), *gas velocity* ( $u_g$ ), *void fraction* ( $\varepsilon_s$ ), *particle diameter* ( $d_p$ ), and *fluid viscosity* ( $\mu_g$ ) were used as model inputs. An example set (see Table S.2) consisting of 108 data vectors/patterns was used in the construction of the model. The  $\beta$  values in the data set were calculated by simulating six drag models proposed by Gibilaro (2001), Gidaspow and Ettihadieh (1983), Syamlal and O'Brien (1987), Arastoopour et al. (1990), Du Plessis (1994) and De Felice (1994). These models predict dissimilar values of the drag coefficient over same parameter ranges. The ranges over which models possess good prediction accuracy are also not specified unambiguously in the literature. Accordingly, in this study a model possessing better drag prediction accuracy than the existing models over a wide range of parameters, has been developed. Here, magnitudes of Reynolds number were varied from  $Re_{mf}$  to  $Re_T$  to compute the corresponding  $\beta$  values. While  $Re_{mf}$  is the value of Reynolds number calculated at minimum fluidization velocity ( $u_{mf}$ ),  $Re_T$  is calculated at terminal velocity ( $u_T$ ). The value of void fraction is varied from fixed bed to lean bed condition. Each model was simulated using a different set of  $Re$  and  $\varepsilon_s$  values falling in the stated range. The  $\beta$  values specified in Table S.2 served as the desired outputs of the GP-based model. For developing this model, the example data set was partitioned into *training* and *test* sets of sizes 81 and 27, respectively. The GP-based model predicting  $\beta$  was developed using *Eureka Formulize* (EF) software package Schmidt and Lipson (2009). This software has been optimized for developing parsimonious models possessing good generalization ability. Towards obtaining an optimal GP-based model, the effects of GP procedural parameters as also the various input normalization schemes, were studied rigorously. The prediction accuracy and the generalization performance of each model was evaluated by computing *coefficient of correlation* ( $CC$ ), and *root mean square error* ( $RMSE$ ), values using the desired and the corresponding model-predicted values of  $\beta$ . These quantities were computed separately for the training

and test data sets. The overall best GP-based drag model was selected on the basis of its high  $CC$  and low  $RMSE$  magnitudes in respect of both training and test data sets. Such an optimal GP-based model for drag ( $\beta$ ) prediction is given as:

$$\beta = 86.2 \cdot \varepsilon_s + \frac{0.785 \cdot \varepsilon_s \cdot Re + 18 \cdot \varepsilon_s^2}{\left(\frac{d_p}{\mu_g}\right) \cdot \varepsilon_g} \quad (6)$$

where  $Re = \frac{d_s |\vec{u}_s - \vec{u}_g| \rho_g}{\mu_g}$ .

The  $CC$  and  $RMSE$  (%) magnitudes pertaining to the predictions by the GP model (Eq. 6) for the training data are:  $CC_{\text{trn}} = 0.675$  and  $RMSE_{\text{trn}}(\%) = 12.1$ , and the corresponding values in respect of the test data are:  $CC_{\text{tst}} = 0.847$  and  $RMSE_{\text{tst}}(\%) = 4.1$ . The relatively high and comparable training and test set  $CC$  values and the corresponding low and comparable  $RMSE$  values indicate good prediction (recall) accuracy and an excellent generalisation performance by the GP-based drag model.

The prediction and generalization performance of the GP-based model was compared with that of the six other models proposed by Arastoopour et al. (1990), Gibilaro (2001), De Felice (1994), Syamlal and O'Brien (1987), Gidaspow and Ettihadieh (1983), and Lundberg and Du Plessis (1994). Table 3 lists the  $CC$  and  $RMSE$  values pertaining to the  $\beta$  predictions made by the stated models using training and test data. It is seen in this table that as compared to other models, the  $CC$  ( $RMSE(\%)$ ) values in respect of the  $\beta$  predictions made by the GP-based model are highest (lowest) for both training and test data. This result indicates that the GP-based model possesses better prediction accuracy and generalization capability than any existing model.

**Table 3:** A comparison of  $\beta$  prediction and generalization performance of various drags models.

Model	Training data		Test data	
	$CC_{\text{trn}}$	$RMSE_{\text{trn}}$ (%)	$CC_{\text{tst}}$	$RMSE_{\text{tst}}$ (%)
Arastoopour et al. (1990)	0.657	12.3	0.751	7.9
Gibilaro (2001)	0.632	14.0	0.682	8.1
De Felice (1994)	0.633	21.7	0.818	6.6
Syamlal and O'Brien model (1987)	0.636	13.6	0.807	7.1
Gidaspow and Ettihadieh (1983)	0.652	12.7	0.718	7.3
Du Plessis (1994)	0.613	16.6	0.822	6.1
GP model (eq. (6))	0.679	12.1	0.847	4.1

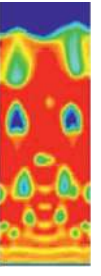
## 4.2 Experimental validation of GP-based drag model

In order to validate the GP-based drag model, experiments were performed using the fluidization set-up shown in Figure 3. Panels (a), (b) and (c) in Figure 4 show the experimental snapshots exhibiting changes in the bed dynamics at three different times, while panels (d), (e) and (f) display the FLUENT-software-simulated contours obtained using the GP-based drag model. The experimental snapshots and the corresponding simulated contours correspond to the gas velocity of 0.13 m/s. The time required to achieve the steady state was three seconds. The time average was carried out from 4 to 15 sec. In the experimental snapshot taken at 0.7 s (Figure 4(a)), two prominent bubbles are seen in the bed followed by a few minor unremarkable ones. The corresponding simulated contours (Figure 4(d)) exhibit a similar trend with a few bubbles in the upper region of the bed. The symmetry of the bubbles is observed when the bed is showing transition from the steady state (fixed bed) to a turbulent state (bubbling bed). After achieving the steady state bubbling, the bubbles showed coalescence and break-down. At 0.9 sec, the bubbles in the experimental snapshot (Figure 4(b)), as also in the contour plot (Figure 4 (e)), can be observed to travel further up in the bed with changes in their sizes; specifically, the right side bubble is more elongated in size than the one on the left. At 1.1 sec the small bubbles in the contour plot (Figure 4(f)), are vanishing due to their bursting at the bed surface; a similar behavior can be seen in the experimental snapshot (Figure 4(c)). As they approach the bed surface, the

bubbles in both the experimental and contour plots are seen to move to the right, appearing to travel faster than other bubbles. From the three contour plots (Figures 4(d), 4(e) and 4(f)), computed using the GP-based drag model, it is observed that they have captured the salient features of the experimentally observed bubble dynamics with a good accuracy. Figure 4 essentially shows that the locations of bubbles in the contours match reasonably well with those in the experiments although the number of bubbles in experiments and contours vary. This could be possibly due to the “wall” effects Altantzis, Bates, and Ghoniem (2015), Li and Benyahia (2012).

## 4.3 Simulation and performance comparison of drag models

The performance of the GP-based drag model in predicting the drag coefficient,  $\beta$ , was compared with the corresponding performance of six other drag coefficient models proposed by, namely, Arastoopour et al. (1990), Syamlal and O'Brien (1988), Gidaspow and Ettihadieh (1983), Gibilaro (2001), De Felice (1994), and Du Plessis (1994). This comparison was made over wide ranges of fluidization parameters namely Reynolds number, gas velocity, particle diameter and voidage. In Figure 5, panels (a) to (e) display plots of the drag coefficient predictions made by the above-stated six models as also the GP-based model for solid volume fraction as a function of the Reynolds number. Here, the magnitude of Reynolds number varies between  $Re_{mf}$  and  $Re_T$ . For all the five particle diameter values (275  $\mu\text{m}$ , 390  $\mu\text{m}$ , 462  $\mu\text{m}$ ,

Experimental snapshot			Simulation using GP-based drag model		
(a)	(b)	(c)	(d)	(e)	(f)
					
0.7s	0.9s	1.1s	0.7s	0.9s	1.1s

**Figure 4:** Comparison of the experimental and GP-model assisted CFD-simulated bubble behavior.

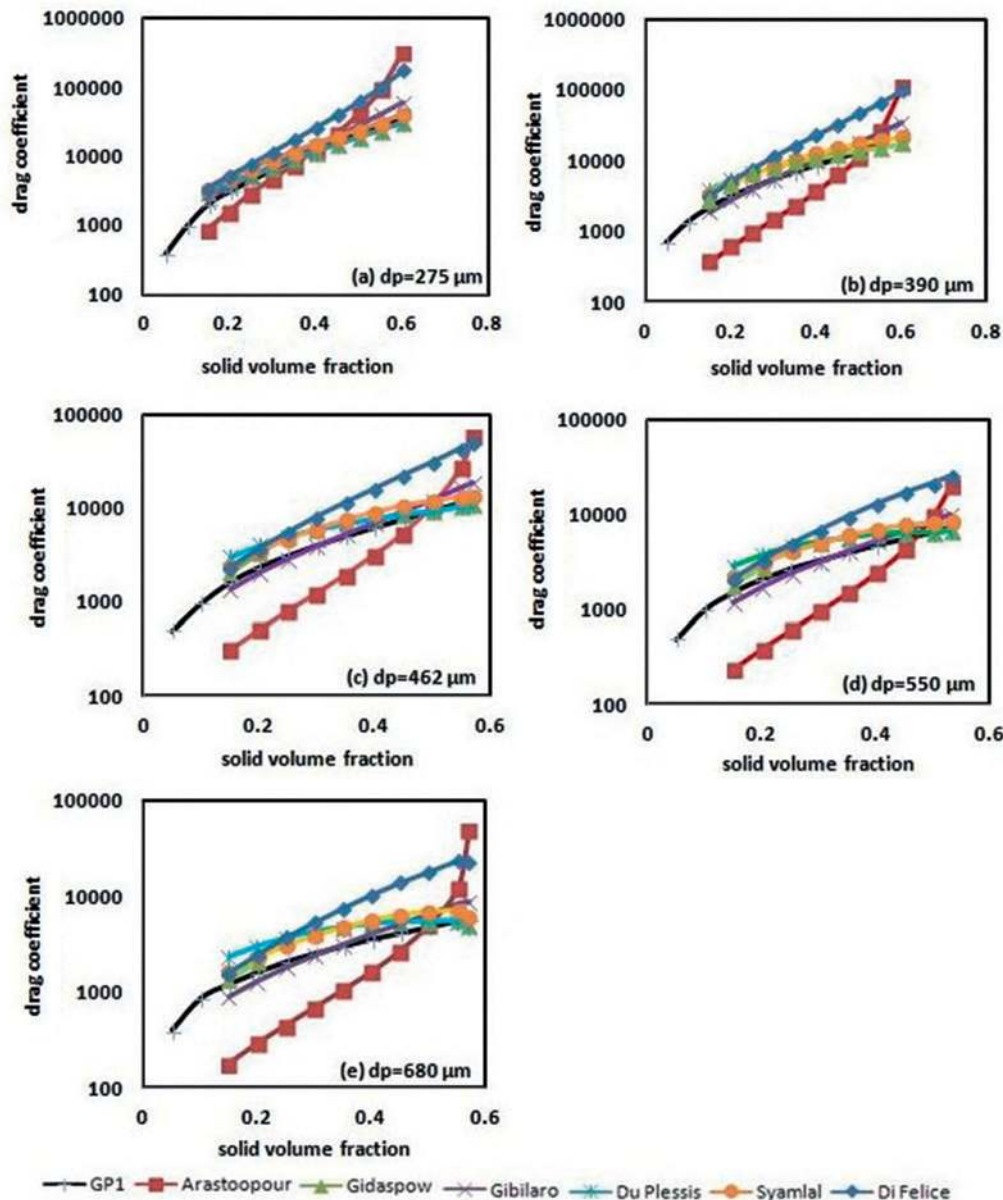
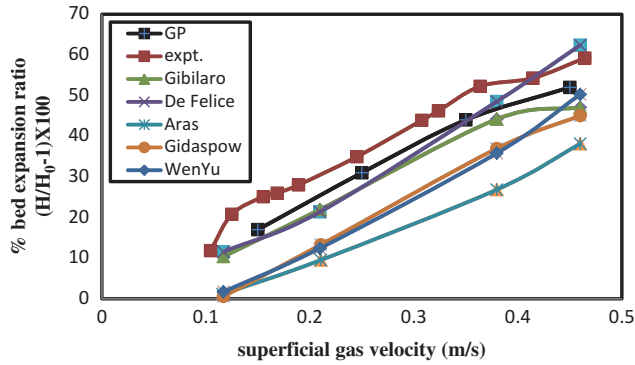


Figure 5: Plots showing the drag coefficient values computed by various models as a function of the solid volume fraction and Reynolds number.

550  $\mu\text{m}$ , and 680  $\mu\text{m}$ ), the GP-model predicted drag coefficient magnitudes are seen to exhibit a trend, which is seemingly an average of the trends displayed by the  $\beta$  predictions by other drag models. Also, for the entire range of Reynolds number considered in the simulations, the prediction of the GP-based drag coefficient model is seen to conform to the trends exhibited by a majority of the existing drag coefficient models.

Figure 6 shows plots of the experimental bed expansion ratio (%) data Vejahati et al. (2009) and the corresponding model predicted ratios as a function of the superficial gas velocity; the said ratios were computed

using the GP-based model as also the models proposed by Arastoopour, Pakdel, and Adewumi (1990), De Felice (1994), Gibilaro (2001), Wen and Yu (1966), and Gidaspow and Ettihadieh (1983). These simulations were performed as described in section 2.3. It can be clearly seen from Figure 6 that the usage of the existing drag models has led to an underestimation of the bed expansion ratio values with the model by Arastoopour, Pakdel, and Adewumi (1990) predicting lowest values of bed expansion ratio. The drag models by Gidaspow and Ettihadieh (1983), and Wen and Yu (1966) have performed similarly in this regard. In is, however, noteworthy that the bed



**Figure 6:** Comparison of the bed expansion ratio simulated using various drag models with the corresponding experimental data.

expansion ratios computed using the GP-based drag model exhibit the closest match with the corresponding experimental ratio magnitudes over the entire range of superficial gas velocity. These results clearly indicate that when compared with the existing models, the GP-based drag coefficient model has provided a superior prediction of the experimentally observed bed expansion ratios. Figure 7 shows a comparison of the experimental Vejahati et al. (2009) and simulated bed pressure drop data. In the beginning of fluidization, there exist large fluctuations in the bed. These large fluctuations weaken substantially when the bed attains a steady-state. Figure 7 shows the steady-state pressure drop values computed using various drag coefficient models as a function of gas velocity. As can be seen in Figure 7, once again the GP-based drag coefficient model shows a better performance than other drag models in providing the closest match with the experimental pressure drop values. The results displayed in Figures (4) to (7) are clearly indicative of the outperformance by the GP- based drag model vis a vis

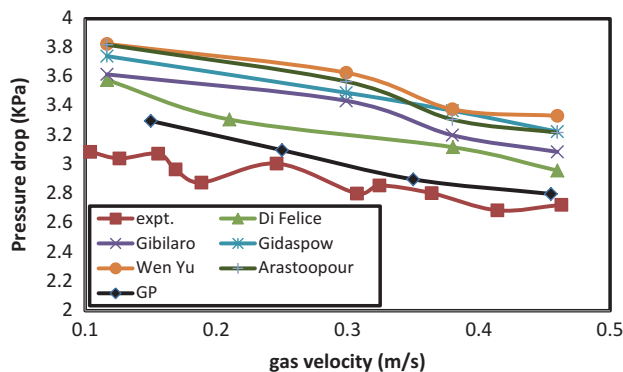


**Figure 7:** Comparison of the experimental steady-state values of the pressure drop inside the bed and the corresponding values computed using various drag models as a function of the gas velocity.

other existing models in predicting the bubble dynamics, bed expansion ratio, and pressure drop values.

## 5 Conclusion

This study uses Geldart's group B particles fluidization data involving wide variations in Reynolds number and solid volume fraction from the studies by Gidaspow and Ettihadieh (1983), Arastoopour et al. (1990), Gibilaro (2001), Du Plessis (1994), Syamlal and O'Brien (1987) and De Felice (1994) to propose a new unified drag model for fluidized beds. An infrequently utilized artificial intelligence based exclusively data-driven formalism, namely, *genetic programming* (GP) has been used to obtain the said model. The novelty of this formalism is that without making any assumptions, it is capable of searching and optimizing both, the structure and associated parameters, of an appropriate linear or nonlinear model that fits a given example input-output data set. Exhaustive simulations were conducted for a 3D bubbling fluidized bed using the proposed GP-based model and its performance was compared with that of a number of existing drag models. The results of this comparison showed that the new drag model exhibits a good agreement with the experimental results pertaining to the pressure drop inside the fluidized bed, and bed expansion. In fact, the GP-based drag model has performed better than the existing models in representing the experimental results involving bed height, pressure drop across the bed, and voidage. Owing to its superior drag prediction ability and applicability over a wide ranges of Reynolds number and solid volume fraction magnitudes, the GP-based model proposed here is capable of gainfully replacing the competing models.

## Notation

$C_d$	drag coefficient
$d_p$	particle mean diameter (m)
$g_0$	radial distribution coefficient
$I$	unity matrix
$I_{2D}$	2nd invariant of the deviatoric stress tensor ( $s^{-2}$ )
$\nabla P$	gas phase pressure drop ( $N/m^2$ )
$\nabla p_s$	pressure drop due to solids ( $N/m^2$ )
$Re$	Reynolds number
$S_k$	strain rate tensor ( $N/m^2$ )
$U_k$	velocity of phase k (m/s)
$v'$	fluctuating velocity (m/s)

**Greek notation**

$\beta$	gas/solid momentum exchange ( $\text{kg/m}^3\text{s}$ )
$\varepsilon_g$	gas volume fraction
$\varepsilon_s$	solid volume fraction
$\eta$	coefficient used in eq. (6) of Table S.1.
$\theta_s$	granular temperature ( $\text{m}^2/\text{s}^2$ )
$\mu_s$	solid viscosity
$\mu_{scoll}$	collisional viscosity (Pa s)
$\mu_{skin}$	kinetic viscosity (Pa s)
$\mu_g$	gas viscosity (Pa s)
$\mu_k$	viscosity of phase k (Pa s)
$\xi_k$	bulk viscosity (Pa s)
$\rho_g$	gas density ( $\text{kg/m}^3$ )
$\tau_g$	gas stress strain tensor (Pa)
$\tau_s$	solid stress strain tensor (Pa)
$\tau_k$	viscous stress tensor ( $\text{N/m}^2$ )
$\phi_s$	transfer rate of kinetic energy ( $\text{kg/s}^3\text{ m}$ )

**Acknowledgments:** SST thankfully acknowledges partial support for this study by *Council of Scientific and Industrial Research* (CSIR), Government of India, New Delhi, under TAPCOAL Network Project.

**References**

- Altantzis, C., Bates, R.B., Ghoniem, A.F., 2015. 3D Eulerian Modeling of Thin Rectangular Gas–Solid Fluidized Beds: Estimation of the Specularity Coefficient and Its Effects on Bubbling Dynamics and Circulation Times. *Powder Technology* 270, 256–270.
- Anderson, T.B., Jackson, R., 1967. Fluid Mechanical Description of Fluidized Beds Equation of Motion. *Ind. Eng. Chem. Fundam.*, 6, 527–39.
- Arastoopour, H., Pakdel, P., Adewumi, M., 1990. Hydrodynamic Analysis of Dilute Gas-Solids Flow in a Vertical Pipe. *Pow. Tech.* 62, 2, 163–170.
- Beetstra, R., A Lattice Boltzmann Simulation Study of the Drag Coefficient of Clusters of Spheres. *Comput. Fluids*, 2006, 35, 966–970.
- Beetstra, R., van der Hoef, M.A., Kuipers, J.A.M., 2007. Drag Force of Intermediate Reynolds Number Flow Past Mono and Bidisperse Arrays of Spheres. *AIChE J.*, 53, 2, 489–501.
- Behjat, Y., Shahhosseini, S., Hashemabadi, S.H., 2008. CFD Modeling of Hydrodynamic and Heat Transfer in Fluidized Bed Reactor. *Int. Commun. Heat Mass.* 35, 357–368.
- Benyahia, S., Syamlal, M., O'Brien, T.J., 2006. Extension of Hill-Koch-Ladd Drag Correlation Over All Ranges of Reynolds Number of Solids Volume Fraction. *Pow. Tech.* 162, 166–174.
- Benzarti, S., Mhiri, H., Bournot, H., 2012. Drag Models for Simulation Gas-Solid Flow in the Bubbling Fluidized Bed of FCC Particles. *World Academy of Science, Eng. Tech.*, 61, 1138–1143.
- Dallavalle, J.M., 1948. *Micrometrics* Pitman, London.
- Davidson, J.F., Harrison, D., 1963. *Fluidized Particles*, Cambridge University Press, New York.
- Davidson, J.F., Harrison, D., 1971. *Fluidization*, 1st edn. Academic press, New York.
- De Felice, R., 1994. The Voidage Functions for Fluid-Particle Interaction Systems. *Int. J. Multiph. Flow.* 20, 1, 153–159.
- Du Plessis, J.P., 1994. Analytical Quantification of Coefficient in the Ergun Equation for Fluid Friction in a Packed Bed. *Trans. porous media* 16, 189–207.
- Du, W., Bao, X., Xu, J., Wei, W., 2006. Computational Fluid Dynamics (CFD) Modeling of Spouted Bed: Assessment of Drag Coefficient Correlations. *Chem. Eng. Sci.*, 61, 1401–1420.
- Enwald, H., Peirano, E., Almstedt, A.E., 1996. Eulerian Two Phase Flow Theory Applied to fluidization. *Int. J. of Multiph. Flow*, 22, 21–66.
- Ergun, S., 1952. Fluid Flow Through Packed Column. *Chem. Prog.* 48, 89.
- Esmaili, E., Mahinpey, N. 2011. Adjustment of Drag Coefficient Correlations in Three Dimensional CFD Simulation of gas-solid bubbling fluidized bed. *Adv. Eng. Software*, 42, 375–386.
- Fattah, K.A., 2012. A New Approach Calculate Oil-Gas Ratio for Gas Condensate and Volatile Oil Reservoirs Using Genetic Programming. *Oil and Gas Business.* 1, 311–323.
- Garside, J., Al-Dibouni, M.R., 1977. Velocity voidage relationship for fluidization and sedimentation. *Ind. Eng. Chem. Proc. Des. Dev.* 16, 206–214.
- Gelderblom, S.J., Gidaspow, D., Lyczkowski, R.W. 2003. CFD Simulations of Bubbling/Collapsing Fluidized Beds for Three Geldart Groups. *AIChE J.* 49, 844–858.
- Ghugare, S.B., Tiwary, S., Elangovan, V., Tambe, S.S., 2014. Prediction of Higher Heating Value of Solid Biomass Fuels using Artificial Intelligence Formalisms. *Bioenergy Research* 7:681–692, doi:10.1007/s12155-013-9393-5.
- Gibilaro, G., 2001. *Fluidization Dynamics*, Butterworth Heinemann.
- Gidaspow, D., Ettihadieh, B. 1983. Fluidization in Two Dimensional Beds with a Jet and Hydrodynamic Modeling. *Ind. Eng. Chem.*, 22, 193–201.
- Hill, R.J., Koch, D.L., Ladd, A.J.C., 2001. Moderate Reynolds Numbers Flows in Ordered and Random Arrays of Spheres. *J. Fluid Mech.*, 448, 243–278.
- Holland, J.H., *Adaptation in Natural and Artificial Systems*. 1975. University of Michigan Press, Ann Arbor.
- Hosseini, S.H., Rahimi, R., Zivdar, M., Samini, A., 2009. CFD Simulation of Gas-Solid Fluidized Bed Containing FCC Particles. *Korean J. of Chem. Engg.* 26, 5, 1405–1413.
- Iaccarino, G., 2001. Predictions of a Turbulent Separated Flow Using Commercial CFD Codes. *J. Fluids Eng.* 123, 819–828.
- Jackson, R., 2000. *The Dynamics of Fluidized Particles*, Cambridge University Press.
- Jenkins, J.T., Savage, S.B., 1983. A Theory for the Rapid Flow of Identical, Smooth, Nearly Elastic, Spherical Particles. *J Fluid Mech.*, 130, 187–202.
- Khandai, D., Derksen, J.J., Van den Akker, H.E.A., 2003. Interphase Drag Coefficients in Gas-Solid Flows. *AIChE J.* 49, 4, 1060–1065.
- Kotanchek, M., 2004. Symbolic Regression via Genetic Programming, in: *Wolfram Technology conference* <http://library.wolfram.com/infocenter/Conferences/5392/> (accessed 03.02.2015).
- Koza, J.R., 1990. Genetically Breeding Populations of Computer Programs to Solve Problems in Artificial Intelligence. In:

- Proceedings of the 2nd International IEEE Conference on Tools for Artificial Intelligence, 6–9 November, 819–827, <http://dx.doi.org/10.1109/TAL.1990.130444>.
33. Kunni, D., Levenspiel, O., 1991. Fluidization Engineering, 2nd Edition Butterworth Heinemann, Boston.
  34. Li, T., Benyahia, S. 2012. Revisiting Johnson and Jackson Boundary Conditions for Granular Flows. *AIChE J* 58, 7, 2058–2068.
  35. Li, T., Pougatch, K., Salcudean, M., Grecov, D., 2008. Numerical Simulation of Horizontal Jet Penetration in a Three Dimensional Fluidized Bed. *Pow. Technol.*, 184, 89–99.
  36. Loha, C., Chattopadhyay, H., Chatterjee, P., 2012. Assessment of Drag Models in Simulating Bubbling Fluidized Bed Hydrodynamics. *Chem Eng. Sci.* 75, 400–407.
  37. Lun, C.K.K., Savage, S.B., Jeffrey, D.J., Chepur, N., 1984. Kinetic theory of granular flow; in elastic particles in a general flow fields. *J. Fluid Mech.* 140, 223–256.
  38. Lundberg, J., Halvorsen, B.M. 2008. A Review of Some Existing Drag Models Describing the Interaction between Phases in a Bubbling Fluidized Bed. *Proc. 49th Scand. Conf. Simulation and Modeling*, Oslo University College, Oslo, Norway.
  39. Mckeen, T., Pugsley, T., 2003. Simulation and Experimental Validation of a Freely Bubbling bed Of FCC Catalyst. *Pow. Tech.*, 129, 1-3, 139–152.
  40. Patil-Shinde, V., Kulkarni, T., Kulkarni, R., Chavan, P.D., Sharma, T., Sharma, B.K., Tambe, S. S., Kulkarni, B. D., 2014. Artificial Intelligence based Modelling of High Ash Coal Gasification in a Pilot-plant Scale Fluidized Bed Gasifier. *Ind. Eng. Chem. Res.*, 53, 49, 18678–18689.
  41. Poli, R., Langdon, W, McPhee, N. 2008. A Field Guide to Genetic Programming. Published via <http://lulu.com> and freely available at <http://www.gp-field-guide.org.uk>.
  42. Richardson, J.F., Zaki, W.N., 1954. Sedimentation and Fluidization, Part I. *Trans. Inst. Chem. Engg.* 32, 82–100.
  43. Rowe, P.N., McGillivray, H.J., Cheesman, D.J., 1979. Gas Discharge from an Orifice into a Gas Fluidized Bed. *Trans. Inst. Chem. Engg.* 57, 194.
  44. Schaeffer, D.G., 1987. Instability in the Evolution Equations Describing Incompressible Granular Flow. *J. Diff. Equation.* 66, 19–50.
  45. Schmidt, M., Lipson, H. 2009. Distilling Free-Form Natural Laws from Experimental Data. *Science* 324, 81–85.
  46. Sharma, S., Tambe, S.S., 2014. Soft-Sensor Development for Biochemical Systems Using Genetic Programming. *Biochem. Eng. J.* 85, 89–100.
  47. Shrinivas, K., Kulkarni, R., Shaikh, S., Ghorpade, R., Vyas, R., Tambe, S.S., Ponrathnam, S., Kulkarni, B.D., 2016. Prediction of Reactivity Ratios in Free Radical Copolymerization from Monomer Resonance-Polarity (Q-e) Parameters: Genetic Programming-Based Models, *Int. J. Chem. React. Eng.* 14(1), 361–372.
  48. Syamlal, M., O'Brien, T.J., 1987. Derivation of Drag Coefficient from Velocity-Voidage Correlation. U.S. Dept. of energy office of fossil energy national energy tech. lab., Morgantown W.V.
  49. Syamlal, M., O'Brien, T.J., 1988. Simulation of Granular Later Inversion in Liquid Fluidized Beds. *Int. J. Multiphase Flow*, 14, 4, 473–481.
  50. Syamlal, M., Rogers, W., O'Brien, T.J. MFIX Documentation, Theory Guide, Technical Note. U.S. Dept. of Energy, Office of Fossil Energy, National Energy Tech. Lab., Morgantown WV, 1993. DOE/METC-94/1004. [https://mfix.netl.doe.gov/download/mfix/mfix\\_legacy\\_manual/Theory.pdf](https://mfix.netl.doe.gov/download/mfix/mfix_legacy_manual/Theory.pdf)
  51. van der Hoef, M.A., van sint Annaland, M., Kuipers, J.A.M., 2005. Computational Fluid Dynamics for Dense Gas-Solid Fluidized Beds: A Multiscale Strategy. *Chem. Eng. Sci.* 59, 51–57.
  52. Vejehati, F., Mahinpey, N., Ellis, N., Nikoo, M.B., 2009. CFD Simulation of Gas-Solid Bubbling Fluidized Bed; A New Method for Adjusting Drag Law. *Canadian J. Chem. Engg.* 48, 19–30.
  53. Wang, J., 2008. High-Resolution Eulerian Simulation of RMS of Solid Volume Fraction Fluctuation and Particle Clustering Characteristics in a CFB Riser. *Chem. Eng. Sci.*, 63, 3341–3347.
  54. Wang, X., Li, Y., Hu, Y., Wang, Y., 2008. Synthesis of Heat-Integrated Complex Distillation Systems via Genetic Programming. *Comput. Chem. Eng.* 32, 1908–1917.
  55. Wen, C.Y., Yu, Y.H., Mechanics of Fluidization, *Chem. Ngg. Prog. Symp.* 1966. Ser 62, 100–111.
  56. Yang, Y., Soh, C.K., 2002. Automated Optimum Design of Structures Using Genetic Programming. *Comp. and Struc.* 80, 1537–1546.
  57. Yang, N., Wang, W., Ge, W., Li, J., 2003. CFD Simulation of Concurrent-Up Gas-Solid Flow in Circulating Fluidized Beds with Structure-Dependent Drag Coefficient. *Chem. Eng J.*, 96, 71–80.
  58. Yi, L., Wanli, K., 2011. A New Genetic Programming Algorithm for Building Decision Tree. *Procedia Eng.* 15, 3658–3662.
  59. Zhang, Y., Reese, J.M., 2003. The Drag Force in Two Fluid Models of Gas-Solid Flows. *Chem. Eng. Sci.* 58, 8, 1641–1644.
  60. Zimmermann, S., Taghipour, F., 2005. CFD Modeling of the Hydrodynamics and Reaction Kinetics of FCC Fluidized Bed Reactors. *Ind. Eng. Chem. Res.*, 44, 9818–9827.
  61. Zinani, F., Philippsen, C.G., Indrusiak, M.L. 2013. Numerical study of gas-solid drag models in bubbling fluidized bed. 22nd International Congress of Mechanical Engineering, November 3-7, Ribeirão Preto, SP, Brazil.

**Supplemental Material:** The online version of this article (DOI: 10.1515/ijcre-2016-0210) offers supplementary material, available to authorized users.